

https://doi.org/10.1070/QEL16514

Study of virtual displays based on raster optical elements

Jaeyeol Ryu, A.N. Putilin

Abstract. **The paper is devoted to the study of the ultimate resolution of virtual displays with raster systems. Raster systems in such displays are used for an essential reduction of their longitudinal overall dimensions. Three schemes are considered: in the first one each element of the raster system forms an image of one pixel only, in the second one each element of the raster system forms a small part of a virtual image, the third scheme is analogous to the first one, but is implemented in the form of a contact lens. For each scheme, we analyse the overall dimensions of the optical system and the characteristics of the virtual image, i.e., the ultimate resolution and the nonuniformity of its illumination.**

Keywords: *raster optics, micromirror rasters, virtual display, contact lens.*

1. Introduction

Raster optics is widely used in optical systems of microscopes, objectives of photo and video cameras, navigation devices, and in virtual displays (VDs) for reducing their overall dimensions [1–4]. A virtual display is a device that produces a virtual magnified image. Virtual displays may be classified with respect to their transparency for the observer eye. If the device is not transparent, i.e. the eye can see only the virtual image, it is called a device of virtual reality. If the device is partially transparent, making it possible for the eye to see simultaneously both the real world and the virtual image, it is called an augmented reality display. In the foreign literature there exist a number of analogous terms, e.g., head-mounted display (HMD), head-up-display (HUD), near-eye-display, virtual reality (VR), etc.

The ultimate goal of VD construction is to create an impression of being in a virtual world, i.e., the VD optical system must produce such a virtual image that a person could not feel the difference between the virtual image and the real world. To this end, VDs must provide high resolution and offer minimal discomfort for the user. Since the VD is placed on the user's head, its overall dimensions and weight are of great importance. In this connection, the application of raster optics for producing the virtual image, used in patent [5], is a good approach to the minimisation of the overall dimensions of VD devices. According to the principles of optical system construction, for the fixed dimensions of the display and position of the observer's eye the overall dimensions of the optical system will increase with increasing required field of view (FoV), and the application of raster systems is expected to allow the longitudinal overall dimensions of the VD to be reduced.

In a number of papers, the following types of raster systems were proposed; 1) an array of spherical short-focus lenses on a planar substrate in front of the display [6]; 2) planar colour holograms writtent with an array of lenses [7]; 3) a raster hologram on a non-planar surface (written with an array of lenses) with a contact lens [8]; and 4) a scheme with a set of holes, each acting as a camera obscura [9]. The above works achieved positive results in the construction of a continuous virtual image with a large FoV and small overall dimensions of the system. In these systems, the arrays of mirrors, lenses, holes, or lens raster microholograms were used as basic elements. Unfortunately, in none of the above papers the ultimate resolution that can be achieved in such systems was estimated.

In the present paper, we describe the optical properties of three basic concepts of raster systems with mirror base elements. Nevertheless the approach proposed makes it possible to estimate the ultimate resolution not only in the systems with mirror (base) elements, but also in the systems with the lens elements.

We first consider a scheme that is very attractive from the engineering point of view. In this scheme each base element of the raster system forms an image of one pixel only. Then we describe the second scheme, in which each base element forms a small part of a virtual image. In the third scheme, we analyse the possibility to create a VD in the form of a contact lens, where the base elements of the raster system are arranged (in analogy with the first scheme).

2. 'One point source–one mirror' scheme

Consider the VD construction where the base element of the raster system is a single point source (PS) (one pixel), placed in front of a concave mirror producing a virtual image. This scheme is partially described in patent [5]. The base element of the system is a mirror, since, in contrast to a lens, it has no chromatic aberrations. If the PS is located at the focal point of the mirror, then its light (after reflection from the mirror surface) will propagate as a parallel beam, i.e., the image of the PS will be located at infinity (Fig. 1).

If several PS's with mirrors are located at a similar distance from the centre of the eye pupil and the angle between the

Jaeyeol Ryu Moscow Institute of Physics and Technology (State University), Institutskii per. 9, 141701 Dolgoprudnyi, Moscow region, Russia; e-mail: Jaeyeol.ryu@phystech.edu;
A.N. Putilin P.N. Lebedev Physical Institute, Russian Academy of Sciences, Leninsky prosp. 53, 119991 Moscow, Russia; e-mail: Putilinan@lebedev.ru

Received 5 September 2017
Kvantovaya Elektronika **48** (1) 87–94 (2018)
Translated by V.L. Derbov

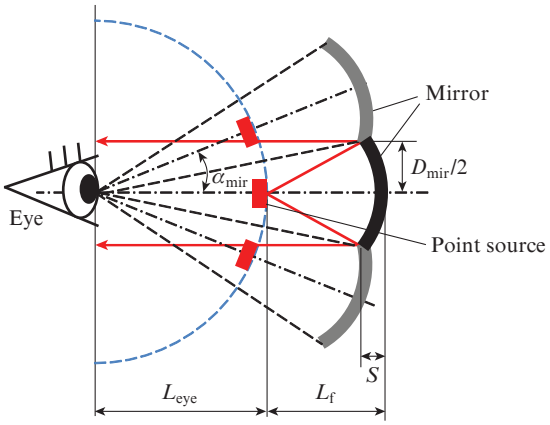

Figure 1. Schematic of the 'one point source–one mirror' system.

axes of the mirrors is α_{mir}, then each PS with the mirror will form a parallel beam. The angles between the adjacent beams will also equal α_{mir}, and each of the beams will be perceived by the eye as a point located at infinity.

Apparently, in order to obtain a maximal number of such virtual points one has to place the mirrors closely, without gaps between them.

From Fig. 1 it follows that

$$\tan\left(\frac{\alpha_{mir}}{2}\right) = \frac{D_{mir}}{2(L_{eye} + L_f - S)}, \tag{1}$$

$$S = R - \sqrt{R^2 - (D_{mir}/2)^2}, \tag{2}$$

where D_{mir} is the mirror diameter; S is the bending deflection of the mirror; L_f is the focal length of the mirror; L_{eye} is the distance from the eye to the point source; and R is the curvature radius of the spherical mirror.

Since for a spherical mirror

$$R = 2L_f, \tag{3}$$

we have

$$\alpha_{mir} = 2\arctan\left[\frac{D_{mir}}{2(L_{eye} - L_f + \sqrt{4L_f^2 - D_{mir}^2/4})}\right]. \tag{4}$$

From Eqn (4), one can determine the diameter of the mirror:

$$D_{mir}(L_{eye}, L_f, \alpha_{mir}) = 2\tan\left(\frac{\alpha_{mir}}{2}\right)\Bigg[(L_{eye} - L_f) \pm \Bigg[L_f^2\left(4 + 3\tan^2\left(\frac{\alpha_{mir}}{2}\right)\right) + 2L_{eye}L_f\tan^2\left(\frac{\alpha_{mir}}{2}\right) - L_{eye}^2\tan^2\left(\frac{\alpha_{mir}}{2}\right)\Bigg]^{1/2}\Bigg]\left[1 + \tan^2\left(\frac{\alpha_{mir}}{2}\right)\right]^{-1}. \tag{5}$$

The density P of PS arrangement in the plane of Fig. 1 equals the number of PS in the unit angle:

$$P = \frac{1}{\alpha_{mir}}. \tag{6}$$

Clearly, the smaller the α_{mir}, the greater the number of PS's that can be integrated in a display of this type, and the smaller can be the mirror diameter D_{mir}. However, it can be decreased only to some limit value, at which the diffraction on the mirror begins to affect the resolution. It is known that the angular diffraction limit of the resolving power is

$$\Psi_{dif} = 1.22\frac{\lambda}{D}, \tag{7}$$

where λ is the light wavelength; and D is the entrance pupil diameter of the optical system (in our case, $D = D_{mir}$).

If for the small mirror diameter Ψ_{dif} exceeds α_{mir}, then it is impossible to resolve two closely spaced PS's, and a further increase in the PS number has no sense. Thus, the angle α_{mir} must be greater than the angular diffraction limit of the resolution:

$$\alpha_{mir} > \Psi_{dif} = 1.22\frac{\lambda}{D_{mir}}. \tag{8}$$

From Eqn (8), one can find the minimal mirror diameter D_{mir}, for which in the scheme of Fig. 1 one can determine the maximal number of PS's (Fig. 2):

$$D_{mir}^{min} = 1.22\frac{\lambda}{\alpha_{mir}}. \tag{9}$$

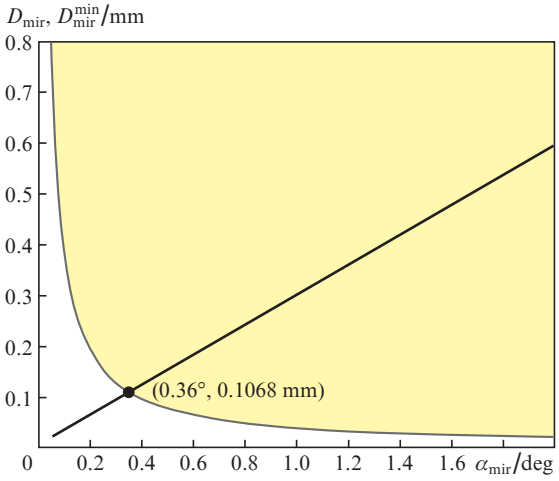

Figure 2. Dependences $D_{mir}(\alpha_{mir})$ for L_{eye} = 15 mm and L_f = 2 mm (black line) and $D_{mir}^{min}(\alpha_{mir})$ for λ = 550 nm (grey curve). The painted area is the region where D_{mir} and α_{mir} satify condition (8).

From the dependences presented in Fig. 2 it follows that for L_{eye} = 15 mm, L_f = 2 mm and λ = 550 nm the optimal mirror diameter is equal to ~0.107 mm, the angle between the mirrors is 0.36° and the angular resolution amounts to 2.8 points deg^{-1}.

Based on ergonomic reasons, let us restrict the distance L_{eye} to the range 10–20 mm, and the focal length L_f to the range 1–5 mm. Figure 3 presents the dependences $\alpha_{mir}(L_{eye}, L_f)$ and $D_{mir}(L_{eye}, L_f)$ calculated for the above ranges of L_{eye} and L_f values. It is seen that the larger the values of L_{eye} and L_f, the smaller the value of α_{mir}. Thus, the 'one PS–one imaging mirror' scheme has a limitation of the number of PS's that can be resolved in the virtual image. Here it is important to note that the size of the elementary optical element should be larger than the eye box (EB):

$$D_{mir} > D_{EB}. \tag{10}$$

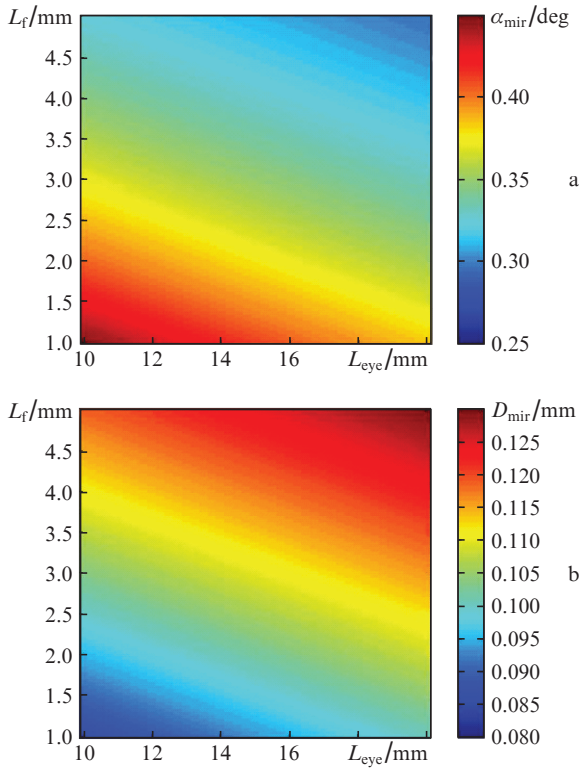

Figure 3. (Colour online) Dependences of (a) the angle α_{mir} and (b) the diameter D_{mir} on L_{eye} and L_f.

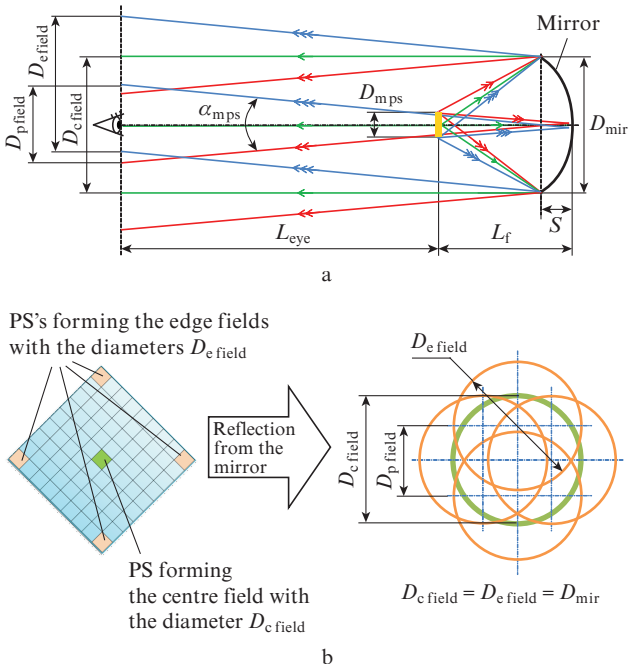

Figure 4. Schematic of (a) the raster system element forming a part of the virtual image with the FoV α_{mps} and (b) the light field spot of the array of PS's placed in the centre and at the ends of diagonals in the plane of the eye pupil at the distance L_{eye} from the PS array after the reflection from the mirror.

As a result, when there is only one PS in the focal point of the optical element, the maximal resolution amounts to approximately three points per one angular degree, provided that $L_{eye} = 10–20$ mm.

3. 'A few pixels per one imaging mirror' scheme

The limitation of the number of PS's per angular degree in the first scheme arises due to the diffraction on the elementary imaging mirror of small diameter.

Now let us consider the case when in front of each mirror there is an array of PS's, i.e., a spatial light modulator (SLM) rather than a single PS. Such mini-arrays of PS's can be integrated into one array with irregular distribution of PS's over the area.

This scheme allows the PS density to be increased with increasing mirror size, since it is possible to add some more PS's in front of each mirror, while the concave mini mirror allows the sources to be resolved according to the Rayleigh criterion [see Eqn (8)]. In contrast to the previous case, each mirror will form a magnified image of the PS array rather than that of a single PS. All elementary mirrors of the raster system together form a large virtual image.

Here it is important to note that the mirror should provide the resolution of each PS in the array. Placing a few PS's in front of each mirror will allow an increase in the diameter of the elementary optical element which can possibly increase the total number of resolved PS's as compared to the previous case for the same distance L_{eye} between the eye and the PS.

Figure 4a presents a schematic of the raster system element that forms a part of a virtual image. In contrast to the first scheme, there is an array of PS's in front of the mirror (Fig. 4b). The Figure also shows the central beam and two edge beams, outgoing from the PS's of the array and located at the centre and the ends of diagonals. These beams form the FoV of the mirror α_{mps}.

The right-hand part of Fig. 4b shows the areas illuminated by four PS's located at the ends of the array diagonals and in the centre at the distance L_{eye} from the PS array after the reflection from the mirror. As seen from the Figure, in order to use up to a half of the light energy from the edge fields with the diameters $D_{e\,field}$, the field diameter $D_{p\,field}$ formed by the crossing of the principal rays from the edge PS's of the array with the plane of the pupil should be smaller than or equal to the diameter of the eye pupil ($D_{p\,field} \leqslant D_{eye}$). The difference of illuminance on the retina due to the beam vignetting by the eye pupil can be compensated for by different brightness of the PS's.

From Fig. 4 it follows that

$$D_{p\,field} = 2(L_{eye} + L_f - S) \times \tan\left[k \arctan\left(\frac{D_{mir}}{2(L_{eye} + L_f - S)}\right)\right], \quad (11)$$

where $k = \alpha_{mps}/\alpha_{mir}$.

To avoid gaps and discontinuities in the virtual image the edges of two adjacent images should either coincide or overlap. The overlap condition for the virtual image of adjacent element of the raster system is determined from the inequality $\alpha_{mps}/2 \geqslant \alpha_{mir} - \alpha_{mps}/2$ (Fig. 5), from which it follows that

$$\alpha_{mps} \geqslant \alpha_{mir}. \quad (12)$$

The key parameters in the study of the considered systems are the mirror diameter, the eye position, and the parameter k.

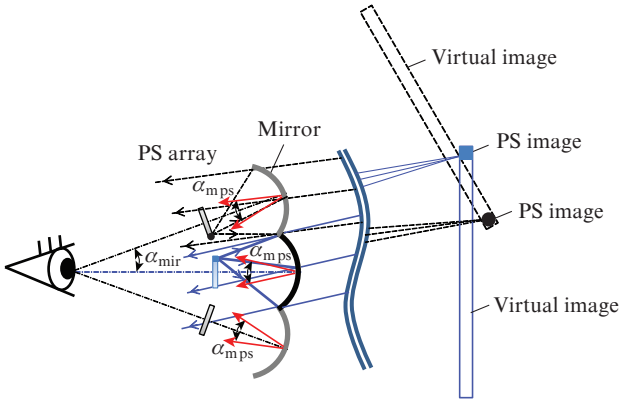

Figure 5. Schematic illustrating the relation between the angles $\alpha_{m\,ps}$ and α_{mir}.

As seen from Fig. 6, the variation of the focal length L_f has almost no effect on the diameter $D_{p\,field}$. However, the greater the D_{mir}, the greater the $D_{p\,field}$. The condition of using a half of the light energy from each PS requires $D_{p\,field} \leqslant D_{eye}$. Since D_{eye} lies in the range 3.5–8 mm, $D_{p\,field}$ must be greater than the minimal size of the eye pupil (3.5 mm). This condition will be fulfilled if $D_{mir} < 2.5$ mm.

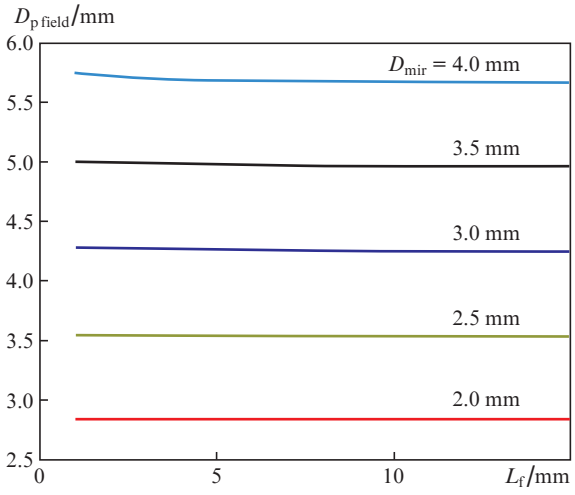

Figure 6. Dependences of $D_{p\,field}$ on L_f at $k = \sqrt{2}$, $L_{eye} = 10$ mm.

To provide a high PS density P and more than a half for the light energy of all PS's transferred to the eye, let us chose the mirror diameter D_{mir} equal to 2.5 mm, the minimal distance L_{eye} equal to 10 mm (because of physiological limitations), and the focal length of the mirror L_f equal to 8 mm. Then the relative aperture of the mirror is $D_{mir}/L_f = 1/3.2$. Then from Eqn (4) and Eqn (11) we obtain $\alpha_{m\,ps} = 11.27°$, $\alpha_{mir} = 7.967°$, $D_{m\,ps} = 2L_f \tan(\alpha_{m\,ps}/2) = 1.578$ mm at $k = \sqrt{2}$. Let us determine the PS density that can be resolved by the considered system.

The criterion of admissible density of the PS arrangement can be found by setting the minimal contrast of the PS array image equal to 0.3, which corresponds to the satisfactory image quality for an average statistical eye:

$$0.3 \leqslant \frac{I_{max} - I_{min}}{I_{max} + I_{min}}. \qquad (13)$$

The corresponding dependences of the modulation transfer function (MTF) or frequency-contrast characteristic of the system are presented in Fig. 7. One can see the contrast level of the image produced by the optical system of objects possessing the appropriate spatial frequencies. Since the mirror system is axially symmetric, it is sufficient to analyse a half of the field from zero to $\alpha_{m\,ps}/2$. From Fig. 7 it follows that this mirror system can transmit the spatial frequencies up to 30.5 points mm^{-1} with a contrast 0.3.

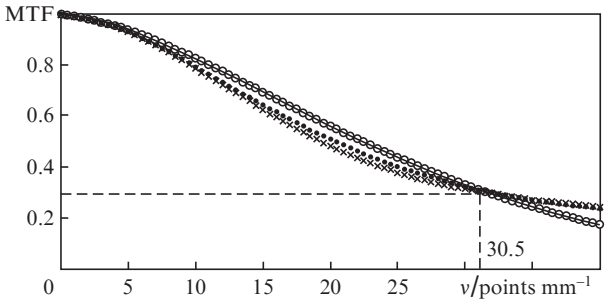

Figure 7. Dependences of MTF on the spatial frequency ν of the PS array for the regions in the centre of the array in the meridional (○) and sagittal (—) plane and for the region of the array at the end of its diagonal in the meridional (•) and sagittal (×) plane. The frequency $\nu_{0.3}$ corresponding to the contrast 0.3 is marked.

Now it is possible to estimate the angular density of the PS for the given value of MTF:

$$P_{ps} = \frac{2\nu_{0.3} D_{m\,ps}}{\alpha_{m\,ps}} = \frac{2 \cdot 30.5 \cdot 1.578}{11.27} = 8.54 \text{ points deg}^{-1}. \qquad (14)$$

In addition, it is possible to count the maximal density N of PS's in the array for the formation of a virtual image with a contrast 0.3 by the system having the FoV $\alpha_{m\,ps}$:

$$N = 2\nu_{0.3} = 2 \cdot 30.5 = 61 \text{ points mm}^{-1}. \qquad (15)$$

We also studied the variation of the optical system resolution depending on the relative aperture and the mirror diameter D_{mir} with the aim to choose the optimal parameters for this scheme. We analysed the PS density P_{ps} per unit angle and the maximal density N of PS's in the array that can be resolved with a contrast 0.3 depending on the relative aperture D_{mir}/L_f and mirror diameter (Fig. 8).

As seen from Fig. 8, the smaller the D_{mir}/L_f, the greater the P_{ps}, i.e., the larger number of PS's can be resolved by our system. For this purpose, it is necessary to increase the PS density N in the array, but in this case the length of the system increases. Note that P_{ps} weakly depends on D_{mir}.

Figure 9 presents the scheme and parameters for calculating the energy of PS light, received by the eye after reflection from the mirror.

Let us denote by E_{θ_Σ} the total light energy from the ith PS that enters the eye. It can be expressed as a sum of the energies E_{1i} and E_{2i}, radiated by the ith PS at negative and positive angles with respect to the system axis and entering the eye.

Assuming that the PS radiates the light beams with Lambert distribution of intensity ($I = I_0 \cos\theta$) the quantity E_{θ_Σ} can be determined as

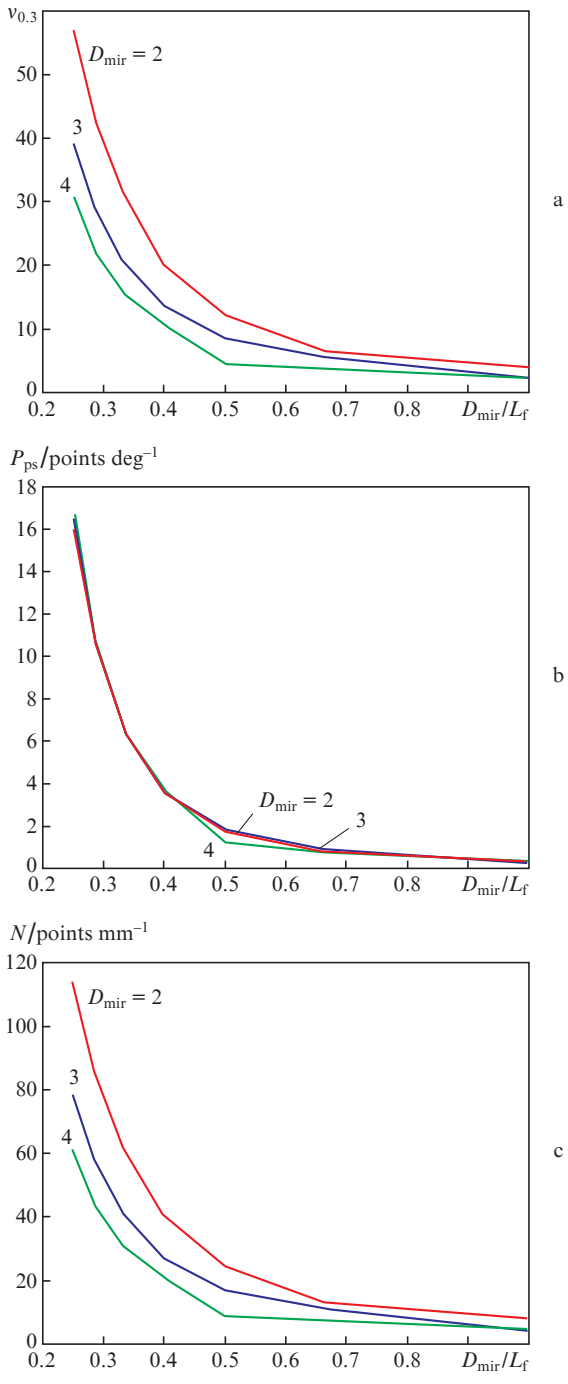

Figure 8. Dependences of (a) $v_{0.3}$, (b) P_{ps} and (c) N on D_{mir}/L_f, corresponding to the image contrast 0.3 on the retina at $k = \sqrt{2}$.

$$E_{\theta_\Sigma}(\alpha_{psi}) = E_{1i}(\alpha_{psi}) + E_{2i}(\alpha_{psi}) = \int_0^{\theta_{1i}} I_0 \cos\theta \, d\theta + \int_0^{\theta_{2i}} I_0 \cos\theta \, d\theta, \quad (16)$$

where I_0 is the intensity of PS light at $\theta = 0$.

As seen from Fig. 9, at some angles α_{psi} the light beam reflected from the mirror is vignetted by the eye pupil. As a result, the image with nonuniform illuminance is formed at the retina.

Figure 10a presents the dependences of the energies E_{1i}, E_{2i} and their sum E_{θ_Σ} on α_{psi} normalised to E_{θ_Σ} at $D_{eye} = 4$ mm. In this case the angular size α_{psi}, corresponding to the uniform

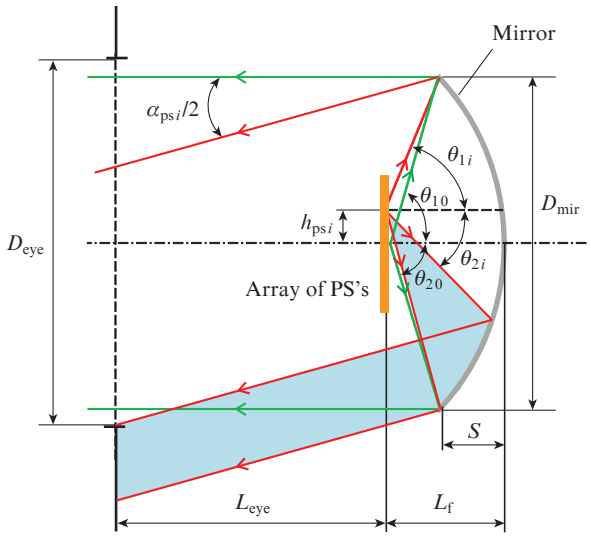

Figure 9. Schematic and parameters for calculating the light energy of the ith PS, entering the pupil. The ultimate rays of the light beam from the ith PS, entering the pupil, make the angles $\theta_{1,2\,i}$. Subscripts 1 and 2 denote the negative and positive angles with respect to the axis of the system; the shaded area is part of the beam vignetted by the pupil.

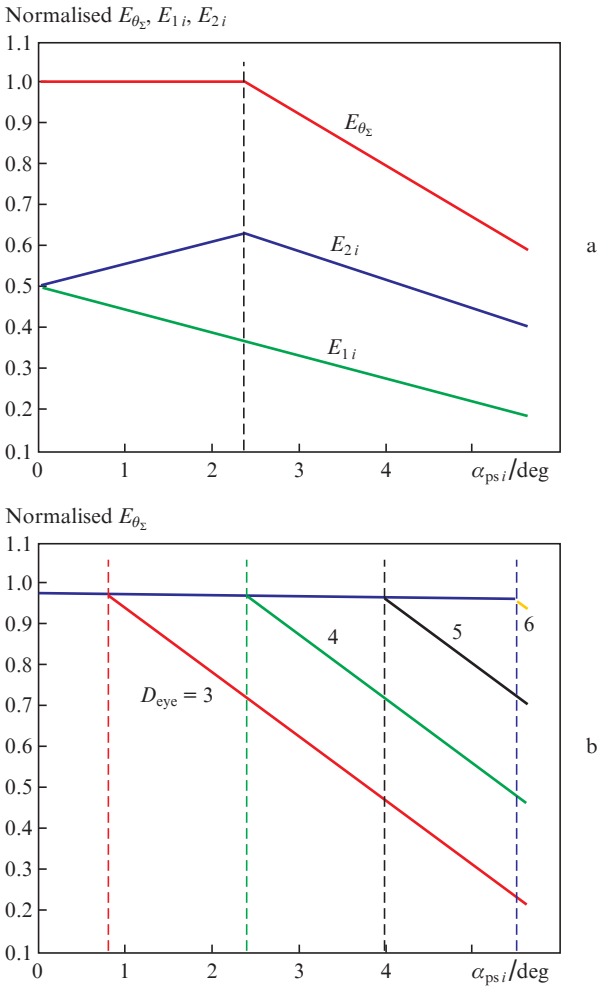

Figure 10. Dependences of (a) the normalised energies E_{1i}, E_{2i} and E_{θ_Σ} for $D_{eye} = 4$ mm and (b) the normalised energy E_{θ_Σ} for $D_{eye} = 3$, 4, 5 and 6 mm on α_{psi}. The dashed lines restrict the angles, corresponding to the uniform illuminance of the images.

distribution of the image illuminance amounts to ~2.3°. Beyond this angle, the illuminance begins to fall. Figure 10b shows that the size of the uniformly illuminated area increases with increasing D_{eye}.

As a result of the study, the optical system with the following parameters was modelled: $D_{eye} = 4$ mm, $D_{mir} = 2.5$ mm, $L_{eye} = 10$ mm and $L_f = 8$ mm (which corresponds to the relative aperture $D_{mir}/L_f = 0.32$). Due to the axial symmetry of the system, it is sufficient to analyse it by considering the rays only in the vertical and horizontal planes.

The modelling using the Zemax programme was carried out for the system of 11 mirrors arranged along the vertical axis and 11 mirrors along the horizontal one, providing the FoV 87.67° = $11\alpha_{mir}$ ($\alpha_{mir} = 7.97°$). As test sources of light we used a set of five emitting rectangular strips (Fig. 11).

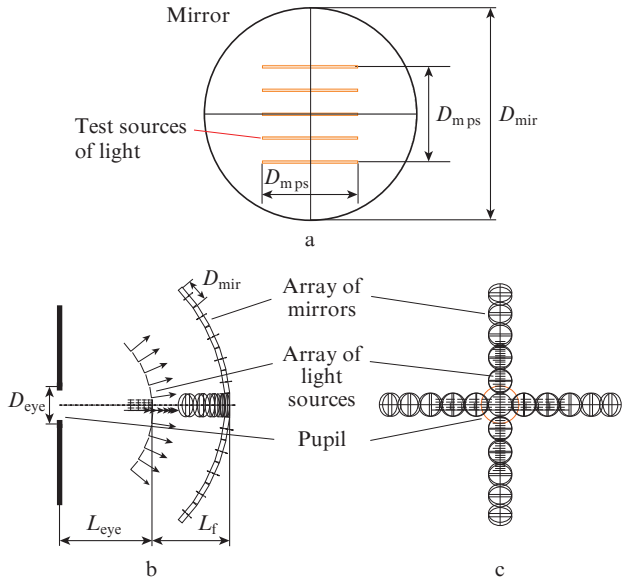

Figure 11. Schematic of multiple sources, showing only those mirrors of the 11×11 array that lie on the vertical and horizontal axes: (a) one mirror with five lines of the light source as a test source; (b) side view (only a small part of the rays shown) and (c) back side.

Figure 12 presents the image of test sources on the retina of the model eye. It is seen that the images formed by the adjacent mirrors appear to be joined.

The modelling has shown that when each mirror of the raster system forms an image of a few PS's, one can increase the PS angular density in the image formed at the retina, as compared to the first scheme. In the particular case when $D_{mir}/L_f = 1/3.2$, $k = \sqrt{2}$, $L_f = 8$ mm, $L_{eye} = 10$ mm, $D_{mir} = 2.5$ mm the density of PS's achieves 8.54 points deg^{-1}, $N = 6$ points mm^{-1}, which corresponds to high-resolution SLM, already developed and produced by industry. In comparison with the first scheme (one PS for each mirror), the resolving power of the VD designed using this scheme can be increased by 3.1 times. In this case, one should provide the possibility to correct the PS brightness for keeping the image illuminance uniform. As mentioned above, the illuminance of the image of each PS on the retina varies depending on the eye pupil size. In this connection, it is necessary to use a system of pupil size monitoring to correct the brightness of the appropriate pixels.

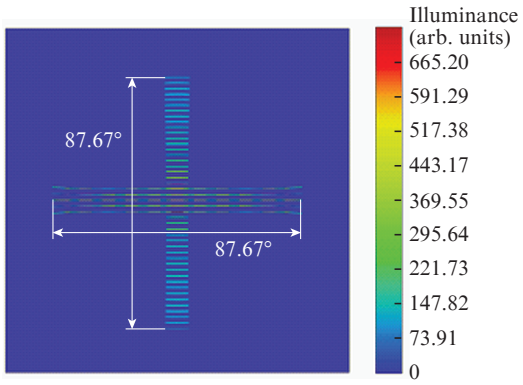

Figure 12. Images of test sources at the eye retina. The maximal incidence angles of rays from PS's on the pupil plane are indicated.

4. 'One point source – one mirror' scheme mounted in a contact lens

Consider one more version of the VD scheme with raster optics, namely, a contact lens placed directly on the eye cornea. A number of electronics-producing companies develop systems with a so-called smart lens [10, 11]. The authors of these papers propose the construction schemes and the multilayer structures of a future smart contact lens, as well as the technology of manufacturing contact lenses with base raster elements [12].

Clearly, one of the most attractive properties of such raster schemes is their small longitudinal size (by definition, contact lenses cannot have the thickness exceeding parts of a millimetre). Therefore, in the present paper we will briefly consider the possibility of mounting the raster optics in a contact lens. Another attractive feature of the contact lens is its location on the eye axis at the minimal possible distance from the pupil. It moves together with the pupil and thus automatically eliminates the necessity to provide a large EB.

Typical parameters of a contact lens are as follows: the diameter, $D_{cl} = 13–15$ mm; the radius of curvature, $R = 8.1–8.9$ mm; and the diameter-to-thickness ratio of the lens, $D_{cl}/t = 20–170$. These parameters are determined, on the one hand, by the human eye physiology (structure, shape, sensitivity of the sclera to the presence of a foreign body on the surface, etc.) and the comfort conditions (water content, oxygen penetration, etc.) of its use, and, on the other hand, by the technology of its fabrication [13–15].

The contact lens is an individual optical system. Each person needs lenses with the parameters depending on the physiological specific features of his eyes. In the present paper, we will estimate the possible maximal resolution of displays based on the contact lenses using some particular parameters of the lenses.

We used the following model (Fig. 13). In the contact lens having a diameter D_{cl} the region having a diameter $D_{cl\,m}$ is selected, containing the base elements, i.e., the raster spherical mirrors with point sources.

Let us determine the maximal FoV α_{max}, equal to the angle between the rays passing through the edges of the pupil and the places of mirror location:

$$\alpha_{max} = 2\arctan\left(\frac{D_{clm} - D_{eye}}{2(L_{cl} - s)}\right), \qquad (17)$$

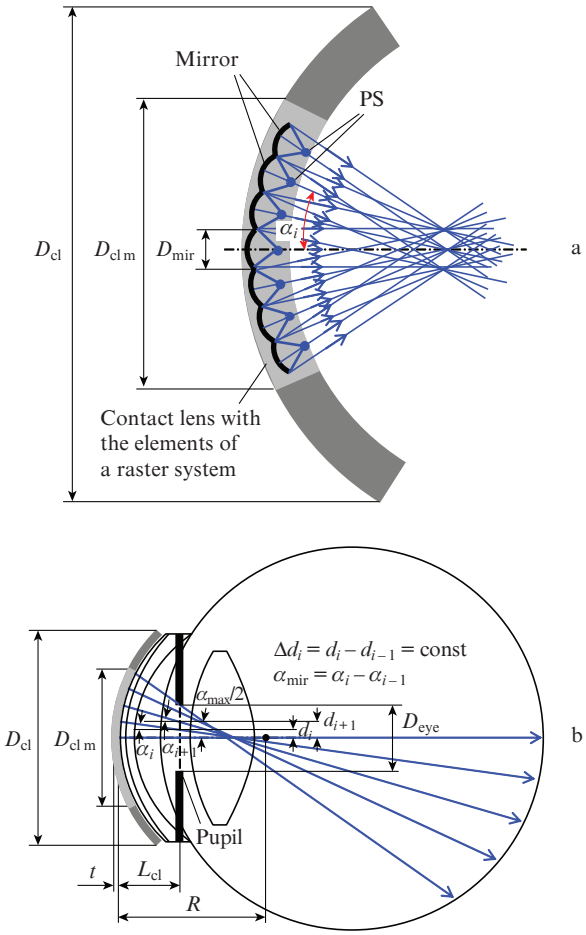

Figure 13. (a) Arrangement of mirrors and the ray paths in a contact lens; (b) the eye and the contact lens with the element of the raster system and the parameters of the model.

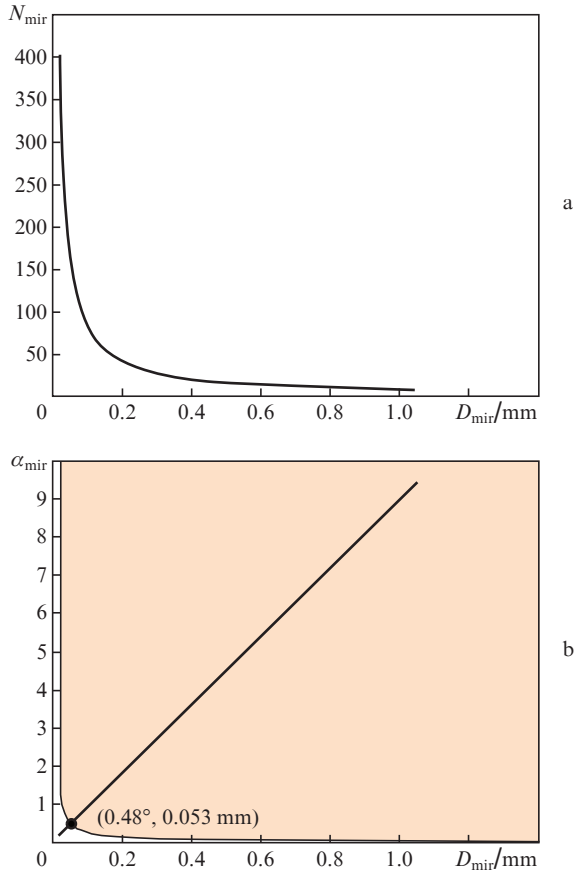

Figure 14. (a) Dependence of N_{mir} on D_{mir} for $D_{eye} = 4$ mm, $D_{cl\,m} = 8$ mm, $R = 8.5$ mm, and (b) dependence of α_{mir} on D_{mir} for the same values of parameters. In the painted area α_{mir} and D_{mir} satisfy condition (8).

where s is the bending deflection of the contact lens part having the diameter $D_{cl\,m}$, in which the elements of the raster system are arranged.

The beams formed by different mirrors will enter the eye at different angles. The greater the distance between the mirror and the contact lens centre, the greater the angle at which the beam formed by this mirror enters the eye pupil. Starting from the optical axis, the pupil is divided into $N_{mir} - 1$ equal segments having the length $d_i - d_{i-1} = \text{const}$, where N_{mir} is the number of mirrors (odd number); d_i is the distance from the boundary of the ith segment to the centre of the eye pupil; i is an integer $[-(N_{mir} - 1)/2 \leqslant i \leqslant (N_{mir} - 1)/2]$; and $d_0 = 0$. The optical axes of the mirror base elements, the number of which is equal to N_{mir}, pass through the boundaries of the appropriate segments. The optical axis of the central mirror passes through the pupil centre, the optical axis of the next mirror passes through the boundary of the first segment, etc., so that the angles between the axes of the adjacent mirrors are $\alpha_{mir} = \alpha_i - \alpha_{i-1} = \alpha_{max}/(N_{mir} - 1)$. Here α_i is the angle between the axis of the contact lens and the axis of the ith mirror.

The diameter of a mirror in the contact lens, D_{mir}, depends on the number of mirrors, N_{mir} (Fig. 14a). To obtain a high-resolution VD, one has to increase N_{mir} maximally, i.e., to reduce D_{mir}. However, with a decrease in the mirror diameter the divergence of the light beam grows due to the diffraction at the mirror. The maximal resolution, estimated in the same way as for the first scheme, i.e., using the Rayleigh criterion (8), with the refractive index of the contact lens material ($n = 1.5$) taken into account, for the given contact lens amounts to two points per angular degree ($1/\alpha_{mir} = 1/0.48° \approx 2$ points deg^{-1}) (Fig. 14b).

The considered model of a contact lens for the virtual display allows a few conclusions. In particular, to reduce the diffraction due to the reflection from the mirror aperture it is desirable to have the mirror diameter no smaller than 53 μm. In this case, according to Fig. 14b, the number of PS's that can be reproduced and resolved by the eye amounts to nearly 156 in the horizontal and the vertical planes in the maximal FoV $\alpha_{max} = 74°$. This means that it is possible to construct a virtual image with the resolution of 2 point per angular degree for the diameter of the eye pupil $D_{eye} = 4$ mm, the diameter of the contact lens with the raster elements $D_{cl\,m} = 8$ mm, and the curvature radius of the contact lens surface R=8.5 mm.

5. Conclusions

Three schemes of the raster virtual display construction are considered. For the first scheme where each mirror produces a virtual image of a single PS it is shown that the PS density (the maximal resolution) can achieve 3 points deg^{-1} in a rather wide FoV (~180°).

The second scheme makes use of one imaging mirror to produce a part of the virtual image field, and the PS density amounts to 8.54 points deg^{-1} in the large FoV (~180°).

The third scheme is analogous to the first one, but the optical system is immersed in the contact lens on the eye cornea rather than located in the air. Using this scheme one can achieve the PS density up to 2 points deg^{-1} in the maximal FoV 74°. This scheme is unique because it is free of EB requirement, which is a weak point in the VD raster systems.

The version of developed virtual displays analogous to the ones considered here in many cases might appear not suitable for the formation of a high-resolution virtual image. However, these schemes still have some positive properties. They would be useful as displays of virtual and augmented reality in indicator and navigation systems, where the produced virtual image should not merge with the surrounding space. The longitudinal size of such displays will be very small and the visual angle, on the contrary, rather large.

References

1. Duparré J., Dannberg P., Schreiber P., Bräuer A., Tünnermann A. *Appl. Opt*., **44** (15), 2949 (2005).
2. Helbing R., Gruhlke R. Patent US 20070181785 A1 (2007).
3. Yu J., Holland D.B., Blake G.A., Guo C. *Opt. Express*, **21** (2), 2097 (2013).
4. Smoot L.S. Patent US 5883606 A1 (1995).
5. Bae Systems PLC, Patent EP 2447758 A1 (2010).
6. Lanman D., Luebke D. *Proc. ACM SIGGRAPH Asia*, **32** (6), 220 (2013).
7. Hong K., Yeom J., Jang C., Hong J., Lee B. *Opt. Lett.*, **39** (1), 127 (2014).
8. Guillaumée M., Vahdati S.P., Tremblay E., Mader A., Cadarso V.J., Grossenbacher J., Brugger J., Sprague R., Moser C. *Proc. SPIE*, **8643**, 864306 (2013).
9. Maimone A., Lanman D., Rathinavel K., Keller K., Luebke D., Fuchs H. *Proc. ACM SIGGRAPH*, **33** (4), 89 (2014).
10. Kim T., Hwang S., Kim S., Ahn H., Chung D. Patent US 20160091737 A1 (2016).
11. Linhardt J.G., Ho H. Patent US 20140197558 A1 (2014).
12. Huang W., Zhao Y. Patent WO 2013081555 A1 (2013).
13. Keirl A., Christie C. *Clinical Optics and Refraction. A Guide for Optometrists, Contact Lens Opticians and Dispensing Opticians* (Oxford: Elsevier Butterworth-Heinemann, 2007).
14. Tasman W. *Duane's Ophthalmology* (Philadelphia: Lippincott Williams & Wilkins, 2012).
15. McNamara N.A., Polse K.A., Brand R.J., Graham A.D., Chan J.S., McKenney C.D. *Am. J. Ophthalmol*., **127** (6), 659 (1999).